NASA TECHNICAL MEMORANDUM

NASA TM X-2580

NASA TM X-2580

COMPARISON OF HEAT TRANSFER CHARACTERISTICS OF THREE COOLING CONFIGURATIONS FOR AIR-COOLED TURBINE VANES TESTED IN A TURBOJET ENGINE

by Frederick C. Yeh, Herbert J. Gladden, and James W. Gauntner

Lewis Research Center
Cleveland, Ohio 44135

NATIONAL AERONAUTICS AND SPACE ADMINISTRATION • WASHINGTON, D. C. • OCTOBER 1972

1. Report No. NASA TM X-2580	2. Government Accession No.	3. Recipient's Catalog No.
4. Title and Subtitle COMPARISON OF HEAT TRANSFER CHARACTERISTICS OF THREE COOLING CONFIGURATIONS FOR AIR-COOLED TURBINE VANES TESTED IN A TURBOJET ENGINE		5. Report Date October 1972 6. Performing Organization Code
7. Author(s) Frederick C. Yeh, Herbert J. Gladden, and James W. Gauntner		8. Performing Organization Report No. E-6948 10. Work Unit No. 501-24
9. Performing Organization Name and Address Lewis Research Center National Aeronautics and Space Administration Cleveland, Ohio 44135		11. Contract or Grant No. 13. Type of Report and Period Covered Technical Memorandum
12. Sponsoring Agency Name and Address National Aeronautics and Space Administration Washington, D.C. 20546		14. Sponsoring Agency Code

15. Supplementary Notes

16. Abstract

A comparison was made of the heat transfer characteristics of three air cooled vanes. The vanes incorporated cooling schemes such as impingement cooling, film cooling, and convection cooling with and without extended surfaces. A redesign study was made for two vanes to improve the cooling effectiveness. An average impingement heat transfer coefficient was calculated on the bases of experimentally determined temperatures at the leading edge and a one dimensional heat transfer calculation. This heat transfer coefficient was compared with existing impingement heat transfer correlations.

17. Key Words (Suggested by Author(s))	18. Distribution Statement
Cooled turbine vanes Film cooling Impingement cooling Heat transfer	Unclassified - unlimited

19. Security Classif. (of this report)	20. Security Classif. (of this page)	21. No. of Pages	22. Price*
Unclassified	Unclassified	36	$3.00

* For sale by the National Technical Information Service, Springfield, Virginia 22151

COMPARISON OF HEAT TRANSFER CHARACTERISTICS OF THREE COOLING CONFIGURATIONS FOR AIR-COOLED TURBINE VANES TESTED IN A TURBOJET ENGINE

by Frederick C. Yeh, Herbert J. Gladden, and James W. Gauntner

Lewis Research Center

SUMMARY

A comparison is made of the heat transfer characteristics of three air cooled vanes tested in a modified J-75 turbojet engine. The comparison is made on the basis of a temperature difference ratio against a coolant- to-gas-flow ratio for both local and average values. A redesign study of two of the vanes shows areas of the vanes which can be significantly improved. Impingement heat transfer coefficients at the leading edges of the three vanes are also compared with existing correlations. The tests were run over the following ranges of conditions: gas temperatures from 1033 to 1650 K (1400° to 2510° F); gas pressures from 19.5 to 29.3 newtons per square centimeter (28.3 to 42.5 psia); coolant temperatures from 300 to 700 K (80° to 800° F); and coolant- to-gas-flow ratios from 0.027 to 0.127.

A film cooled vane having air injected near the leading edge pressure surface, even when used with ineffective internal convection cooling, is shown to be more effective than a fin augmented, convection cooled vane having a fin effectiveness factor of 3. The film cooling advantage is also noted far downstream, near the trailing edge. A film cooled vane having air injected near the leading edge suction surface is shown to be less effective in the midchord region than a fin augmented, convection cooled vane. Film cooling air exiting from the suction surface holes is ineffective and may even have a detrimental effect on the cooling of the suction surface trailing edge.

A comparison was made on the impingement heat transfer characteristics of the vanes. The comparison confirms that the ratio of the distance between the impingement nozzles and the heat transfer surface to the equivalent slot width is important for obtaining optimum impingement cooling. The maximum to minimum temperature difference, the hot spot temperature, and the average temperature of the vanes can be reduced by design modifications which are discussed.

Experimental leading edge impingement heat transfer coefficients are compared within ±10 percent of existing correlations for the three vanes studied.

INTRODUCTION

The heat transfer performance of three air cooled turbine stator vanes was investigated in a modified J-75 turbojet engine. Correlations of temperature data from these vanes are compared to illustrate the cooling efficiency for various cooling concepts.

Much attention has been devoted to the general problem of cooling turbine vanes because of the trend towards higher operating turbine temperatures in turbojet engines. Various cooling schemes have been used to keep the metal temperatures within safe operational limits. The vane designs reported herein incorporate cooling concepts of impingement cooling, film cooling, and convection cooling with and without finned surfaces. A comparison of these cooling configurations and their effects on the metal temperatures could serve as a guide to the design of other air cooled turbine vanes.

Methods for correlating experimental metal temperatures for turbine vanes and blades were reported in references 1 to 3. These references report that a correlation of the temperature difference ratio (ratio of gas minus metal temperature to gas minus coolant temperature) with the coolant flow to gas flow ratio was as good as, or better than, the more complicated correlations considered. This type of correlation is used herein as the means for comparing vanes investigated. Impingement heat transfer correlations from references 4 to 6 are used to compare heat transfer coefficients calculated from experimental temperature data by means of a one dimensional heat transfer analysis.

The purposes of this report are (1) to compare the cooling effectiveness of three air cooled vanes tested at the Lewis Research Center, (2) to modify the designs so as to improve their cooling effectiveness, and (3) to compare the impingement cooling heat transfer coefficients with some existing correlations.

Test procedures and data used in the correlations are reported in references 3 and 7. Test conditions for the vanes were provided by a modified high pressure spool from a J-75 turbojet engine. This research engine and the supporting facilities are described in reference 8. Test data were obtained for the following ranges of conditions: turbine inlet temperatures from 1033 to 1650 K (1400° to 2510° F); coolant inlet temperatures from 300 to 700 K (80° to 800° F); coolant- to-gas-flow ratios from 0.027 to 0.127; and turbine inlet pressures from 19.5 to 29.3 newtons per square centimeter (28.3 to 42.5 psia).

VANE DESCRIPTION

Two of the vanes compared in this report were designed by NASA and fabricated from Udimet 700, a nickel based alloy. The third vane, of commercial origin, was cast MAR M302. The vanes had a span length of about 10.2 centimeters (4 in.) and a

chord length of about 6.4 centimeters (2.5 in.). The external dimensions of the vanes were identical. The differences were in the internal configurations required to achieve the desired cooling scheme. In all cases, the cooling air entered the vane from supply tubes located at the vane tip.

Vane A

A cutaway view of vane A is shown in figure 1. Cooling air enters a central cavity in the vane and then divides to flow in two directions. A portion of the air flows towards the leading edge through a row of 46 impingement holes to cool the vane leading edge. These impingement cooling holes are 0.127 centimeter (0.050 in.) in diameter, spaced 0.203 centimeter (0.080 in.) apart, and located about 0.66 centimeter (0.26 in.) from the leading edge surface. The cooling air, after impinging on the internal leading edge surface, flows in the chordwise direction and exits through film cooling holes located about 1.78 centimeters (0.7 in.) downstream from the stagnation point. The film cooling holes on the suction surface are a single row of 59 holes, 0.064 centimeter (0.025 in.) in diameter and spaced 0.158 centimeter (0.062 in.) apart, oriented at a 28° angle to the vane surface. Two rows of holes staggered with respect to each other are located on the pressure surface. These rows contain 58 and 59 holes, respectively, 0.071 centimeter (0.028 in.) in diameter, spaced 0.158 centimeter (0.062 in.) apart. Both rows are oriented at 40° angles to the vane surface.

The cooling air not used for impingement cooling enters a series of chordwise passages formed by capped fins which are integral with the vane suction and pressure surfaces. The fin passages begin midway between the leading and trailing edges of the vane and extend to the end of the central plenum chamber. There are 92 chordwise passages along each vane surface. The passages are 0.076 by 0.076 centimeter (0.030 by 0.030 in.) in cross section. The length of the fin passages is about 2.2 centimeters (0.87 in.) on the suction surface and about 1.8 centimeters (0.71 in.) on the pressure surface. The fins are 0.025 centimeter (0.010 in.) thick. Cooling air from the pressure and suction surfaces combines at the end of the fin passages and exits through the split trailing edge. The width of this split trailing edge passage is 0.051 centimeter (0.020 in.).

Vane B

A cutaway view of vane B is shown in figure 2. It is similar to vane A in many respects. Cooling air enters a central cavity in the vane and then divides to flow in two

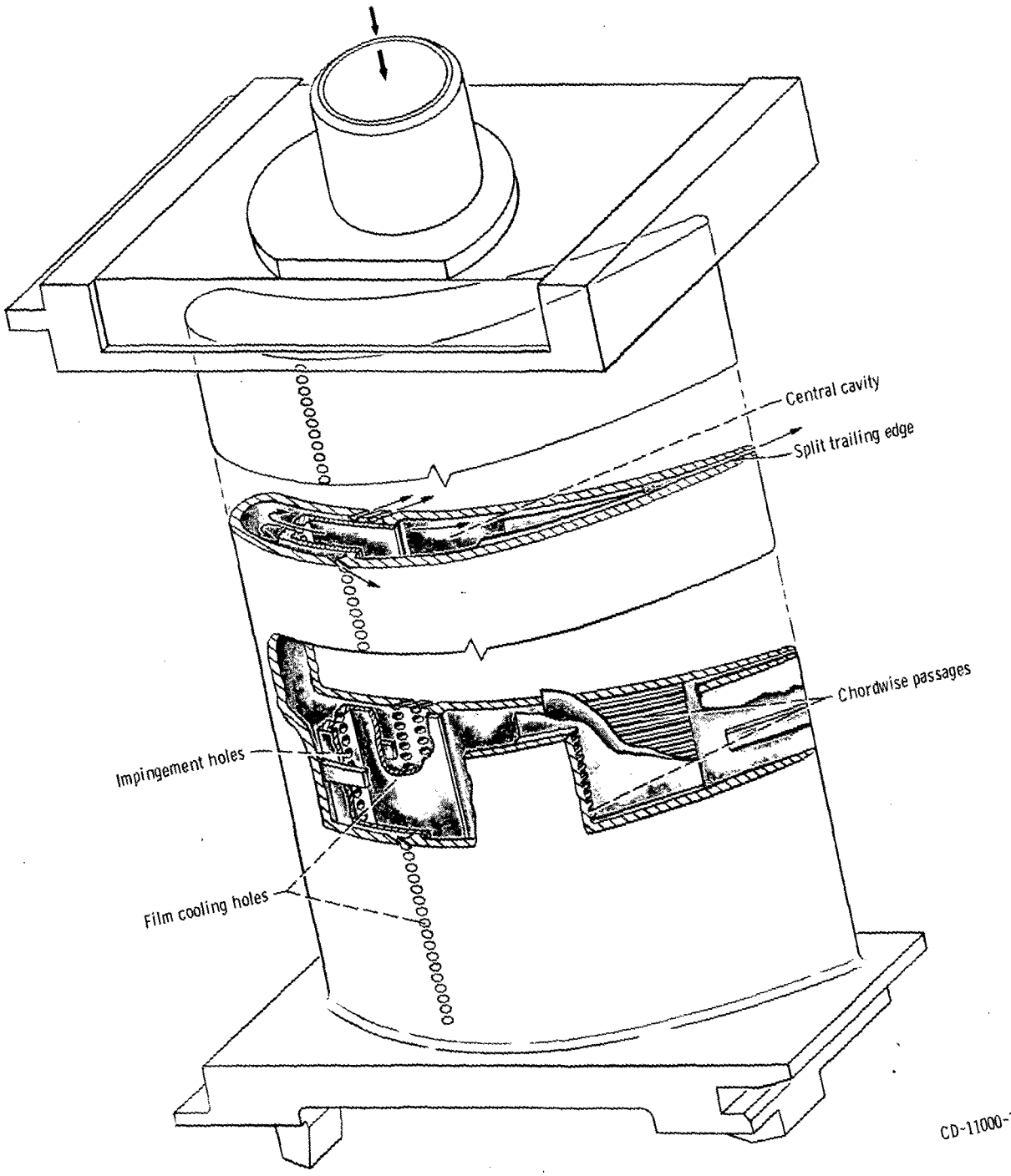

Figure 1. - Cutaway view of vane A.

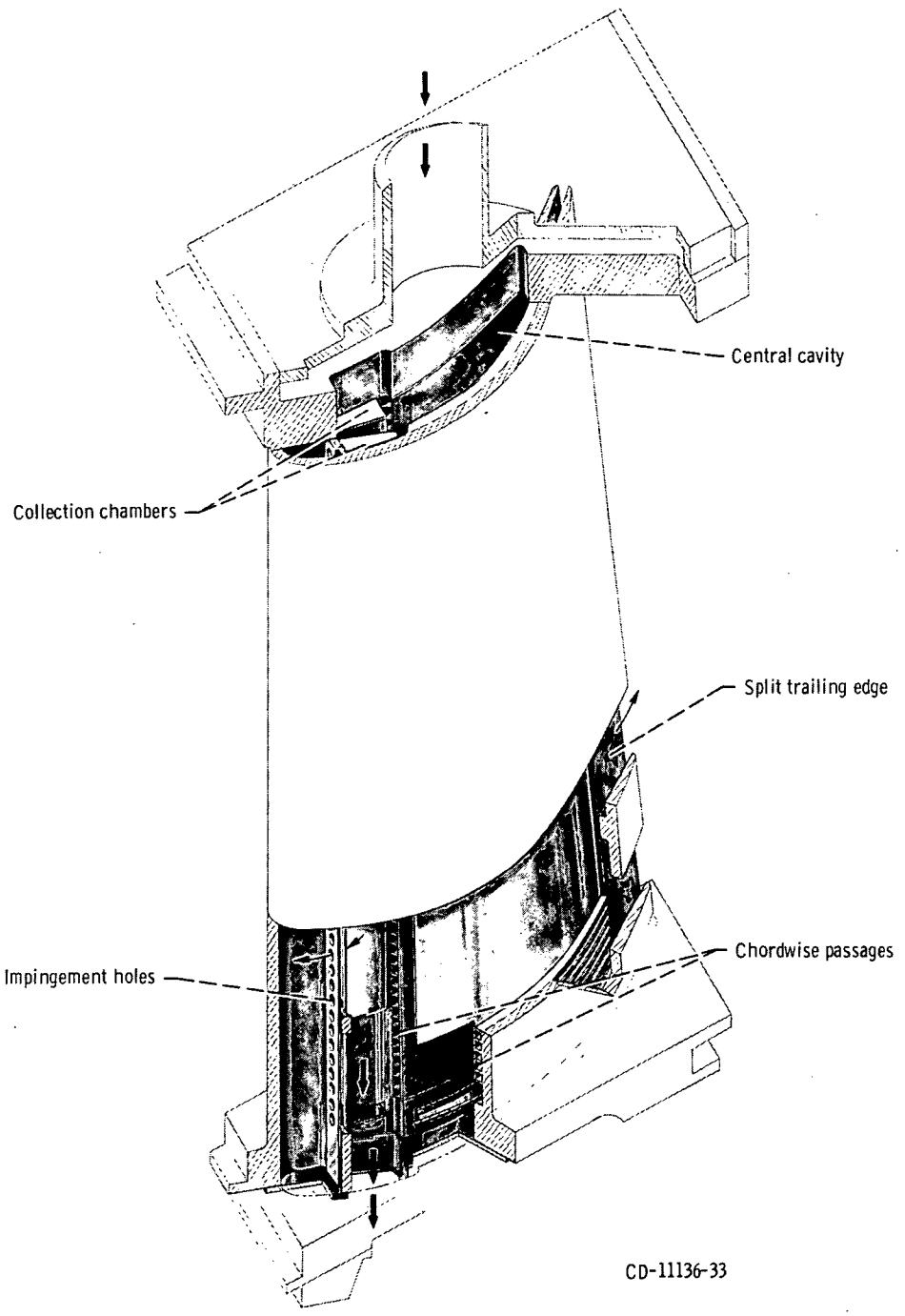

Figure 2. - Cutaway view of vane B.

directions. A portion of the air flows through a row of 46 impingement holes to cool the leading edge. These holes are 0.127 centimeter (0.050 in.) in diameter, spaced 0.203 centimeter (0.080 in.) apart, and located 0.51 centimeter (0.20 in.) from the leading edge surface. Unlike in vane A, the impingement air flows into two collection chambers immediately aft of the leading edge and exits at the vane hub. There are no film cooling holes in vane B.

The cooling air not used for impingement cooling enters a series of chordwise passages formed by capped fins which are integral with the vane suction and pressure surfaces. The fin passages begin immediately aft of the impingement exit air collection chambers and extend to the end of the central plenum chamber. There are again 92 chordwise passages along each surface. The passages are 0.076 by 0.076 centimeter (0.030 by 0.030 in.) in cross section. The lengths of the fin passages are about 3.63 centimeters (1.43 in.) on the suction surface, and about 3.23 centimeters (1.27 in.) on the pressure surface. The fins are 0.025 centimeter (0.010 in.) thick. Like in vane A, the midchord cooling air from the pressure and suction surfaces combines and exits through the split trailing edge. The width of this split trailing edge is 0.076 centimeter (0.030 in.).

Vane C

A cutaway view of vane C is shown in figure 3. Vane C's leading edge and most of the pressure and suction surfaces are cooled by impingement cooling. Film cooling slots are located at the trailing edge so that the trailing edge is cooled by both film cooling and convection cooling. Cooling air enters the vane and flows into a vane tip plenum chamber, at which point the flow divides. Part of the air flows into a leading-edge impingement tube and impinges on the internal surface of the vane leading edge. The impingement tube has 16 impingement slots, each 0.47 centimeter (0.184 in.) long and 0.020 to 0.038 centimeter (0.008 to 0.015 in.) wide and located about 0.145 centimeter (0.057 in.) from the leading edge surface. The surface area in this leading edge region is increased by chordwise fins. This flow then passes between the fins, around the leading edge impingement tube in a chordwise direction, and exhausts into the leading edge collector tube. The remainder of the flow in the tip plenum chamber enters a midchord supply tube and flows toward the vane hub. This air then impinges on the internal surfaces of the vane suction and pressure sides by flowing through 481 holes on the suction side and 334 holes on the pressure side. The hole diameter is 0.038 centimeter (0.015 in.). This flow then exits through film cooling slots on the pressure and suction surfaces and through the split trailing edge. On the pressure surface, the film cooling air flows through a continuous slot, 9.27 centimeters (3.65 in.) by 0.065 centimeter

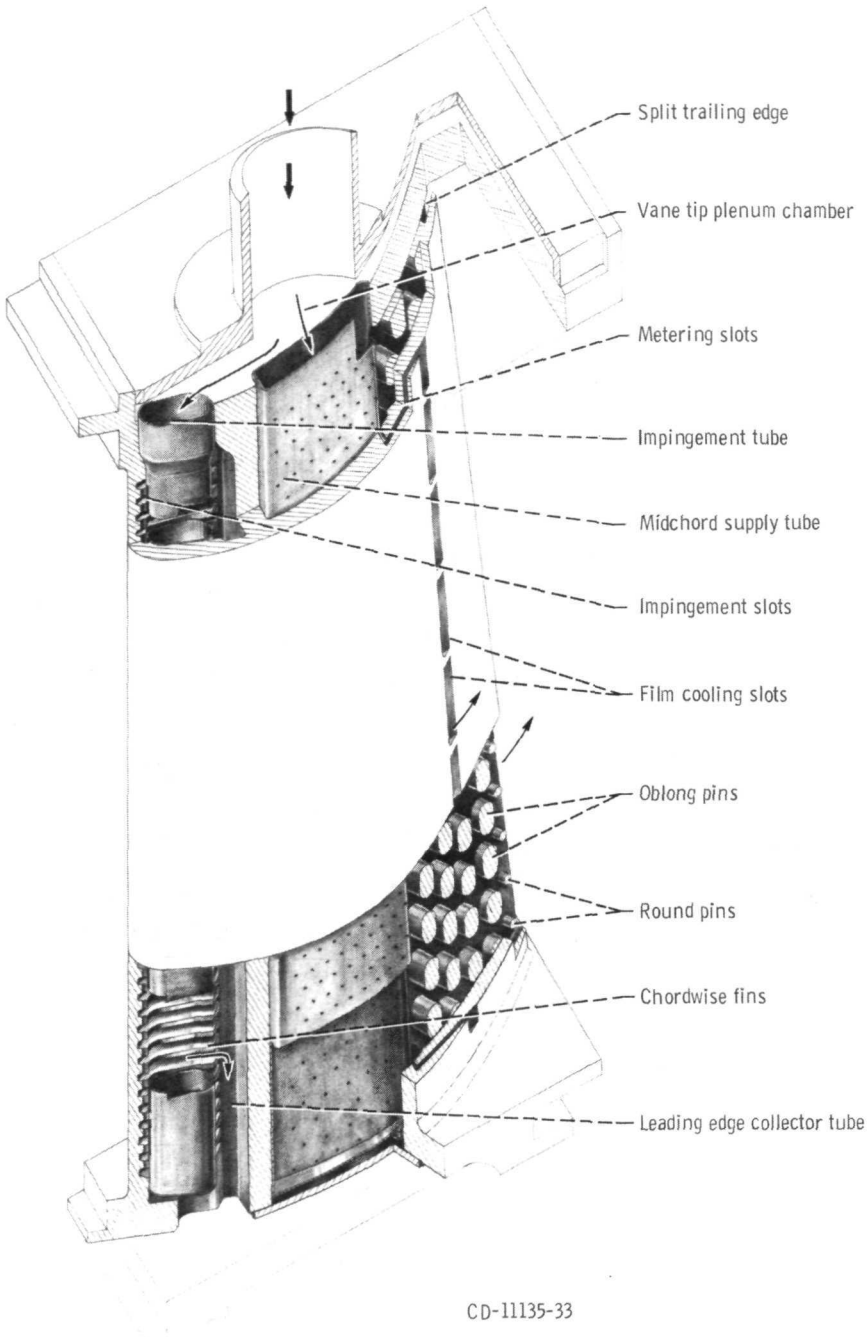

Figure 3. - Cutaway view of vane C.

(0.025 in.), which is fed by 16 metering slots, each of which is 0.25 centimeter (0.10 in.) by 0.053 centimeter (0.021 in.). On the suction surface, film cooling air flows through eight slots, 1.11 centimeters (0.438 in.) by 0.051 centimeter (0.020 in.). The trailing edge contains a staggered array of pin fins consisting of four rows of oblong pins and one row of round pins. The oblong pins are 0.38 centimeter (0.15 in.) by 0.25 centimeter (0.10 in.) in cross section. Since the split trailing edge is tapered, the oblong pins vary in height from 0.18 centimeter (0.070 in.) to 0.094 centimeter (0.037 in.). The round pins have a diameter of 0.20 centimeter (0.080 in.) and a height of 0.064 centimeter (0.025 in.).

VANE INSTRUMENTATION

For each of the three vane configurations tested, a set of five instrumented vanes was used. Most of the thermocouples were concentrated at the midspan position because the midspan plane of the airfoil was considered as the "test section." The midspan thermocouples were distributed over three test vanes located in the center of the five vane cascade.

Twenty-five thermocouples were used for vane A. Fourteen of these were located at 13 positions around the vane at the midspan plane. (Two of the thermocouples were located at the leading edge for redundancy.) The remaining 11 thermocouples on the vane hub and tip were used to monitor the vane temperature during engine testing. A composite of the midspan plane thermocouples for vane A is shown in figure 4(a).

Because of the close similarity between vane A and vane B, vane B was thermocoupled identically to vane A. Twenty-five thermocouples were again used. Fourteen of these were located at 13 positions around the vane at the midspan plane. A composite of the midspan plane thermocouples for vane B is shown in figure 4(b).

Seventeen thermocouples were used for vane C. Fifteen of these thermocouples were located at 9 positions around the vane at the midspan plane. Some of the thermocouple locations were different from those of vanes A and B. A composite of the midspan thermocouples for vane C is shown in figure 4(c).

METHODS OF ANALYSIS

Comparison of Cooling Effectiveness

Several methods for correlating experimental data were examined in references 1 to 3. It was shown that a correlation of the temperature difference ratio

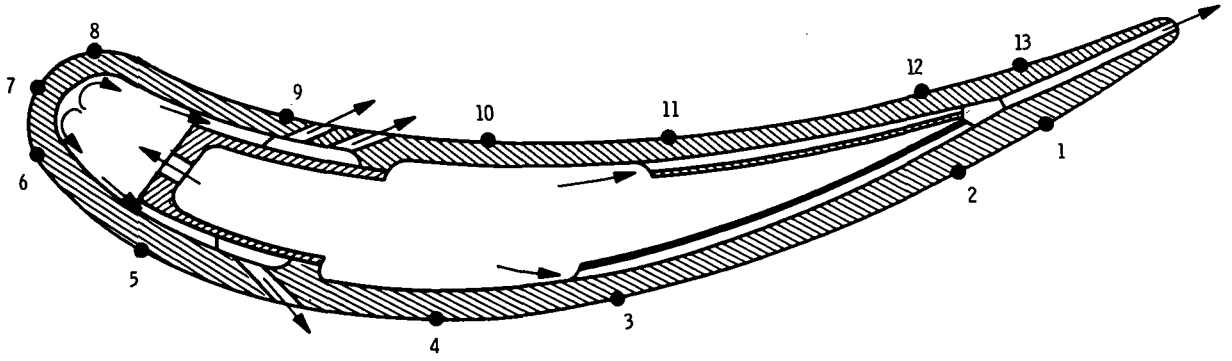

(a) Vane A. Impingement cooled leading edge; convection and film cooled pressure and suction surfaces; chordwise fins in midchord region.

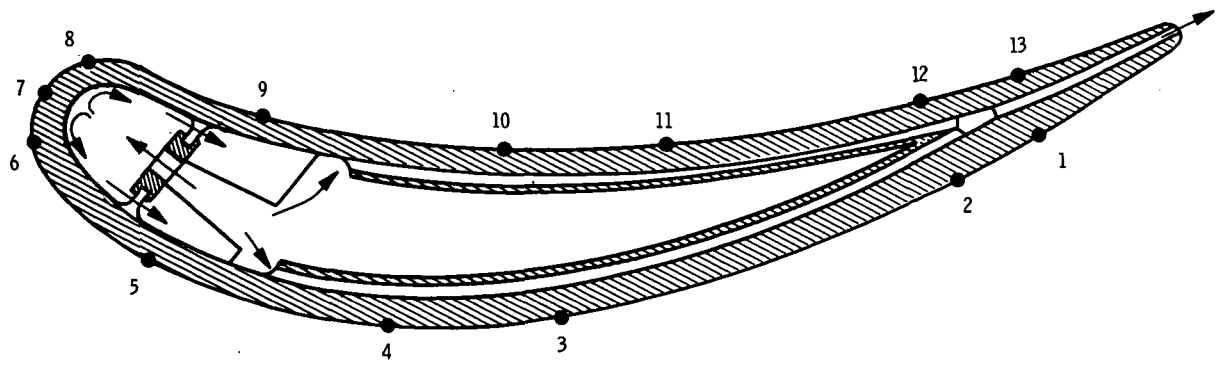

(b) Vane B. Impingement cooled leading edge; convection cooled pressure and suction surfaces; chordwise fins in midchord region.

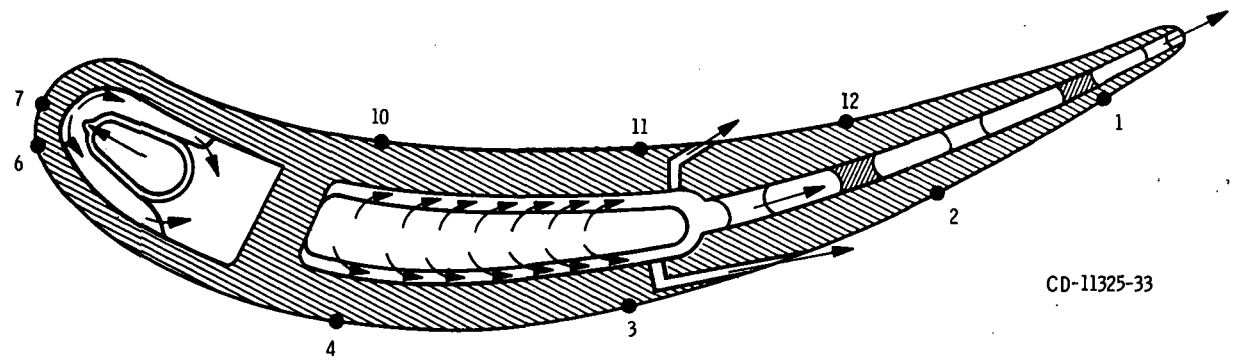

(c) Vane C. Impingement cooled and chordwise finned leading edge; impingement cooled pressure and suction surfaces; convection and film cooled trailing edge.

Figure 4. - Typical cross sections (not to scale) showing cooling schemes and midspan thermocouple locations (numbers) of three test vanes.

$(T_{ti} - T_w)/(T_{ti} - T_{ci})$, commonly referred to as φ, against the coolant- to-gas-flow ratio w_c/w_g was satisfactory. The symbols are defined in the appendix. The relation between the temperature difference ratio φ and the coolant- to-gas-flow ratio w_c/w_g takes the form

$$\varphi = \frac{1}{1 + A\left(\frac{w_c}{w_g}\right)^B} \tag{1}$$

where A and B are constants obtained from a least square fit of the experimental data, w_g is the gas flow per vane channel, and w_c is either the total coolant inlet flow per vane or the local coolant flow through a certain part of the vane.

While there are certain assumptions and simplifications in this type of correlation, the error involved is negligible for the data presented (refs. 3 and 9). This correlation is a useful tool for comparing the cooling effectiveness of different vane and blade designs tested in the same facility. In this report, the φ values obtained from the curve fit of experimental data are used in comparing the cooling effectiveness of the vane designs. The comparison is limited to the vane midspan region, where most of the thermocouples are located. Comparisons are made on the basis of local temperatures to evaluate the effect of the vane design on that particular location, as well as on the basis of an integrated average metal temperature over the midspan region in order to compare the overall performance of the vane.

Impingement Heat Transfer Coefficient Comparison

Impingement heat transfer correlations. - Impingement cooling heat transfer has received increasing attention in turbine cooling. Numerous correlations are now available. This report compares experimental data from the three vanes tested with modifications of the correlatings given in references 4 to 6. The following are the correlations, rearranged in comparable forms for comparison:

From reference 4

$$\frac{\bar{h}2b_{es}}{k} = 0.36\left[\frac{G2b_{es}}{\mu}\right]^{0.62}\left[\frac{l}{b_{es}}\right]^{-0.38} \tag{2}$$

From reference 5

$$\frac{\bar{h}2b_{es}}{k} = 0.355\left[\frac{G2b_{es}}{\mu}\right]^{0.73} Pr\left[\frac{l}{b_{es}}\right]^{-0.52} \tag{3}$$

From reference 6, for $c_n/d_n = 1.67$

$$\frac{\bar{h}2b_{es}}{k} = 0.870\left[\frac{G2b_{es}}{\mu}\right]^{0.614} Pr\left[\frac{l}{b_{es}}\right]^{-0.475}\left[\frac{2b_{es}}{D_h}\right]^{0.386} \tag{4}$$

From reference 6, for a 0.064 centimeter (0.025 in.) slot

$$\frac{\bar{h}2b_{es}}{k} = 0.820\left[\frac{G2b_{es}}{\mu}\right]^{0.585}\left[Pr\,\frac{l}{b_{es}}\right]^{-0.410}\left[\frac{2b_{es}}{D_h}\right]^{0.415} \tag{5}$$

It should be noted that in reference 4 the Reynolds number is written as $Re = 2\rho V_a l/\mu$, where V_a is the velocity of the jet arriving at the target surface if the target were not there. However, reference 4 showed that if the ratio of $z_n/d_n \leq 4$, then $V_a = V_n$, where V_n is the velocity at the nozzle exit. For the vanes under consideration, the value of $z_n/d_n = 4$. Therefore, for the purpose of this comparison, ρV_a can be replaced by G_n.

The heat transfer coefficients obtained from equations (3) to (5) are average values based on optimum nozzle location relative to the target surface. Reference 5 presents curves which show the variation of heat transfer coefficient as a function of the ratio of target distance to equivalent slot width (z_n/b_{es}). These curves are used in conjunction with equations (3) to (5) to correct for the nonoptimum nozzle to surface distance of vanes A, B, and C. Reference 6 presents various correlations for different geometries tested. Two equations from reference 6 are also used for comparison - one having a c_n/d_n value closest to that of the test vanes being compared, and the second having a slot width closest to the equivalent slot width of these vanes.

Coolant side and gas side heat transfer coefficients. - The ratio of the gas side heat transfer coefficient to the coolant side heat transfer coefficient can be obtained by a simple heat balance. Assuming negligible temperature drop across the metal wall,

$$h_g S_o(T_{ti} - T_w) = h_c S_i(T_w - T_c) \tag{6}$$

or

$$\frac{h_g}{h_c} = \frac{S_i}{S_o}\left(\frac{T_w - T_c}{T_{ti} - T_w}\right) \tag{7}$$

By neglecting the difference between T_c and T_{ci}, it can be shown from equation (1) that

$$\frac{h_g}{h_c} = \frac{S_i}{S_o}\left(\frac{1 - \varphi}{\varphi}\right) \tag{8}$$

For a cylinder,

$$h_c = \frac{h_g}{\frac{r_i}{r_o}\left(\frac{1 - \varphi}{\varphi}\right)} \tag{9}$$

The local experimental coolant heat transfer coefficient can be determined if the experimental gas side heat transfer coefficient is known. Reference 7 presents experimental data showing the ratio of the gas side heat transfer coefficient in the research engine to the gas side heat transfer coefficient in the four vane cascade ($h_{g,eng}/h_{g,cas}$). In the vicinity of the leading edge, the ratio is shown to be about 1.30. For the leading edge area, the gas side heat transfer coefficient in the cascade is determined by the equation for flow around a cylinder, which is

$$h_{g,cas} = 1.14(Re_f)^{0.5}(Pr_f)^{0.4}\left[1 - \left|\frac{\theta}{90}\right|^3\right]\frac{k_f}{D_{le}} \tag{10}$$

where the characteristic dimension in the Reynolds number is the diameter of the leading edge, and the property values are based on the film temperature which is defined as the average of the total turbine inlet temperature and the wall temperature. The gas side heat transfer coefficient for the engine is then calculated by using the equation

$$h_{g,eng} = 1.30\, h_{g,cas} \tag{11}$$

Finally, by using equations (9) to (11), a local coolant side Nusselt number can be calculated for the three leading edge thermocouple locations, if the value of θ for each is known and if the properties are based on the inlet coolant temperatures:

$$Nu_x = \frac{h_{c,eng,x}\, 2b_{es}}{k_{ci}} \tag{12}$$

An average Nusselt number is calculated over the area bounded by thermocouple locations 6 and 8 on figure 4(a) by using Simpson's rule:

$$Nu = \frac{1}{6}\left(Nu_{\theta_1} + 4Nu_{\theta_0} + Nu_{\theta_2}\right) \tag{13}$$

where θ_1 refers to the suction surface side, θ_0 refers to the leading edge, and θ_2 refers to the pressure surface side.

Vane Potential

For a given ratio of coolant flow to gas flow, the maximum turbine inlet temperature (T_{ti}) that can be used in an engine is often limited by the maximum permissible metal temperature of the turbine vane. The following expression for the gas temperature can be obtained from equation (1):

$$T_{ti} = T_w + \frac{T_w - T_{ci}}{A\left(\frac{w_c}{w_g}\right)^B} \tag{14}$$

where A and B are again constants obtained from a least squares curve fit of the experimental data points. From equation (14), the maximum permissible turbine inlet temperature can be calculated for the maximum permissible metal temperature and coolant inlet temperature if the experimental correlation of φ against w_c/w_g is known for that location.

Modification of vane design. - The cooling effectiveness of the vanes compared in this report can be improved by lowering the metal temperature of the vane at the hottest locations while maintaining an acceptable temperature gradient in the chordwise direction. This can be accomplished by adjusting the flow distribution between the vane lead-

ing edge and trailing edge regions, by extending the chordwise fins in the midchord pressure and suction surfaces, and by optimizing the spacing between the impingement nozzles and the leading edge surface.

Effect of modifications on metal temperatures. - An expression for determining the effect of these modifications on the vane metal temperature can be derived by using equations (8) and (1). For a constant gas side heat transfer coefficient, equation (8) can be written as

$$h_g = h_{c,1} \frac{S_i}{S_o} \left(\frac{1 - \varphi}{\varphi} \right)_1 = h_{c,2} \frac{S_i}{S_o} \left(\frac{1 - \varphi}{\varphi} \right)_2 \tag{15}$$

Rearranging equation (15) and using equation (1) yields

$$\left(\frac{1 - \varphi}{\varphi} \right)_2 = \frac{h_{c,1}}{h_{c,2}} \left(\frac{1 - \varphi}{\varphi} \right)_1 = \frac{h_{c,1}}{h_{c,2}} A \left(\frac{w_c}{w_g} \right)_1^B \tag{16}$$

from which

$$T_{w,2} = T_{ti} - \frac{T_{ti} - T_{ci}}{1 + \frac{h_{c,1}}{h_{c,2}} A \left(\frac{w_c}{w_g} \right)_1^B} \tag{17}$$

Equation (17) shows that to calculate the effect of vane modification on the vane metal temperature, it is necessary to know the ratio of the original coolant side heat transfer coefficient to the modified heat transfer coefficient.

Numerous correlations are available for impingement heat transfer coefficients and for convective heat transfer coefficients for extended surfaces. For the purpose of this report, curves from reference 5 which show the relative heat transfer coefficient as a function of the ratio of target distance to equivalent slot width are used for the impingement heat transfer calculations. For the pressure and suction surfaces, where fins are extended to cover previously unfinned areas, the following equation from reference 10 is used:

$$\frac{h_{c,2}}{h_{c,1}} = \frac{h_{fin}}{h_i} = \left[\frac{2 \tanh \psi \, L_{fin}}{\psi} + m_{fin}\right] \frac{1}{m_{fin} + \tau_{fin}} \tag{18}$$

where $\psi = (2h_i/k_w\tau_{fin})^{1/2}$

RESULTS AND DISCUSSION

Coolant Flow Distribution

In order to compare experimental heat transfer data for vanes having different cooling configurations, it is necessary to know the coolant flow distribution inside the vanes. A detailed flow distribution measurement, using ambient temperature air, was made for each of the three vane configurations. The procedure for determining the flow distribution is reported in reference 3. Results of the flow distribution for vane A, taken from reference 3, are reproduced here as figure 5. The results from a similar flow distribution test for vane B are shown in figure 6. Data reported in reference 11 are used to obtain figure 7 for vane C. Each of these three figures show the percentage of the total coolant flow which exits through a particular region of the vane into the gas stream as a function of the ratio of coolant inlet pressure to turbine inlet pressure.

As can be seen from figure 5, vane A cannot be operated below a pressure ratio of 0.88. Below this value, hot gas will be drawn into the vane through the pressure sur-

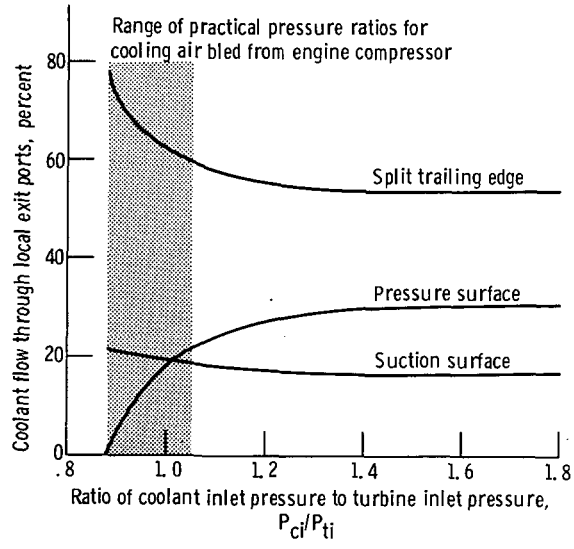

Figure 5. - Percent of coolant flow through vane A exit ports as a function of pressure ratio. (Data from ref. 3.)

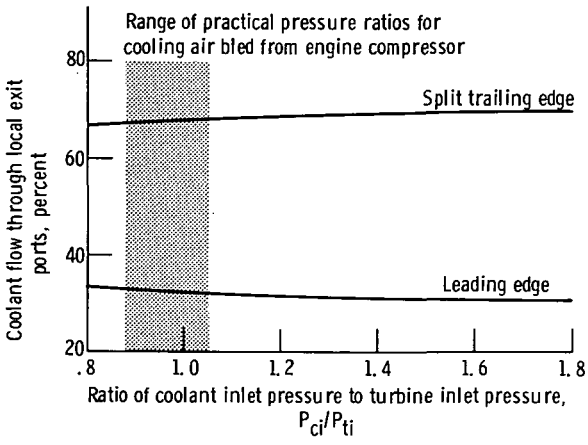

Figure 6. - Percent of coolant flow through vane B exit ports as a function of pressure ratio.

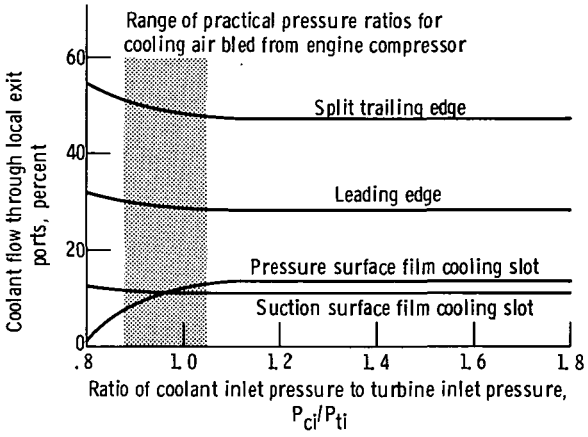

Figure 7. - Percent of coolant flow through vane C exit ports as a function of pressure ratio. (Data from ref. 11.)

face film cooling holes. The ratio of total coolant flow to gas flow at which this pressure ratio occurs is temperature dependent. At a cooling air temperature of 922 K (1200° F), this pressure ratio occurs at a total-coolant- to-gas-flow ratio of 0.02. Similarly, figure 7 shows that vane C cannot be operated below a pressure ratio of 0.79, which corresponds to a total-coolant- to-gas-flow ratio of 0.003 at 922 K (1200° F). No limitation is shown for vane B, since all of the coolant air exits to about the same external pressure level.

At a pressure ratio of 1.0, which is where the vanes will be usually operated, both vanes A and C have approximately the same flow through the suction and pressure surface film cooling holes. At this same pressure ratio, the percentages of the total coolant flows through the split trailing edges for vanes A, B, and C are 63, 68, and 48, respectively. The percentages of total flows through the impingement nozzles of the three

vanes are 37, 32, and 29, respectively. The compressor of the engine cannot supply cooling air above a pressure ratio of 1.05. For this reason, the shaded areas in figures 5 to 7 indicate the practical range of pressure ratios for cooling air bled from the engine compressor.

Comparison of Local Temperature Difference Ratio

As was mentioned in the section titled METHODS OF ANALYSIS, the comparison of the cooling effectiveness of the vanes is based on the experimental correlation of the temperature difference ratio φ against the ratio of coolant flow to gas flow w_c/w_g. The gas flow w_g is the flow through the engine per vane channel. For the coolant flow w_c, either the local flow ratio to the region of the vane under consideration or the total flow ratio to the vane can be used in the correlation. This is done in order to compare the effectiveness of each type of cooling scheme for a given amount of local coolant flow and to demonstrate the end result of a particular vane design for a given amount of total coolant flow. All thermocouples on vanes A, B, and C have been correlated according to equation (1) against both local and total coolant flow ratios. The corresponding correlation constants appear in tables I and II, respectively. Only representative correlations based on local coolant flow ratios are discussed in the following paragraphs. Small arrows are used in figure 8 to indicate the design ratio of total coolant flow to gas flow of 0.05 at a coolant inlet temperature of 922 K (1200° F) for each vane. The maximum coolant- to-gas-flow ratio shown for each curve in figure 8 represents a total-coolant-to-gas-flow ratio of 0.10 for each vane.

Leading edge φ values. - Figure 8(a) shows the local φ values at the leading edge stagnation point, plotted against the local coolant flow ratio to the leading edge. All three vanes used impingement cooling at the leading edge. Vane C, which incorporates plate fins at the leading edge and also the most optimum nozzle location relative to the leading edge surface, has the highest φ values which, for similar gas and coolant conditions, indicates that vane C has the lowest wall temperature. The local φ values of vane A are lower than those of vane B, which in turn are lower than those of vane C.

There are no chordwise plate fins in the leading edge of either vane A or B. The leading edge designs of these two vanes are identical except that the impingement nozzles of vane B are located closer to the leading edge surface than are those of vane A. The more optimum location of the impingement nozzles of vane B accounts for the better cooling effectiveness. Reference 5 shows that for impingement cooling, with a nozzle centerline spacing (c_n/d_n) of 1.67, optimum heat transfer is obtained when the value of z_n/b_{es} is about 2. The heat transfer coefficient decreases as the value of z_n/b_{es} increases. The value of z_n/b_{es} for vanes C, B, and A are 6.5, 8.2, and 10.6, respectively.

TABLE I. - CORRELATION CONSTANTS BASED ON LOCAL-COOLANT-TO-GAS-FLOW RATIO (w_c/w_g) FOR LOCAL TEMPERATURE-DIFFERENCE-RATIO (φ_x) CORRELATION EQUATION

$$\varphi_x = \frac{1}{1 + A\left(\frac{w_c}{w_g}\right)^B}$$

Thermocouple location, x (a)	Vane	Correlation constant		Thermocouple location, x (a)	Vane	Correlation constant	
		A	B			A	B
1	A	0.1812	-0.54	8	A	0.1455	-0.63
	B	.1403	-.56		B	.1105	-.65
	C	.0580	-.76		C	------	-----
2	A	0.1429	-0.44	9	A	0.2108	-0.42
	B	.0476	-.65		B	.1706	-.46
	C	.0464	-.73		C	------	-----
3	A	0.0459	-0.58	10	A	0.0009	-1.65
	B	.0561	-.55		B	.0865	-.50
	C	.0602	-.60		C	.0685	-.71
4	A	0.0321	-0.80	11	A	0.0094	-0.97
	B	.0731	-.51		B	.0675	-.59
	C	.0898	-.67		C	.0544	-.67
5	A	0.0309	-0.87	12	A	0.0169	-0.94
	B	.1261	-.55		B	.0784	-.61
	C	------	-----		C	.0082	-1.20
6	A	0.0163	-1.23	13	A	0.0451	-0.88
	B	.0994	-.66		B	.1934	-.53
	C	.2160	-.46		C	------	-----
7	A	0.2664	-0.62				
	B	.1581	-.63				
	C	.1796	-.48				

[a]The location numbers are not related to any specific locations on the vane surfaces. The specific location of each thermocouple on each vane can be determined from fig. 4 together with fig. 10, 11, or 12.

TABLE II. - CORRELATION CONSTANTS BASED ON TOTAL-COOLANT-TO-GAS-FLOW RATIO (w_c/w_g) FOR LOCAL TEMPERATURE-DIFFERENCE-RATIO (φ_x) CORRELATION EQUATION

$$\varphi_x = \frac{1}{1 + A\left(\frac{w_c}{w_g}\right)^B}$$

Thermocouple location, x (a)	Vane	Correlation constant		Thermocouple location, x (a)	Vane	Correlation constant	
		A	B			A	B
1	A	0.2753	-0.48	8	A	0.1215	-1.03
	B	.1553	-.60		B	.4017	-.59
	C	.1135	-.72		C	------	-----
2	A	0.2643	-0.41	9	A	0.1252	-0.87
	B	.0945	-.66		B	.4100	-.45
	C	.0875	-.71		C	.1516	-.72
3	A	0.1187	-0.49	10	A	0.0180	-1.25
	B	.0885	-.61		B	.1347	-.53
	C	.1007	-.61		C	.1158	-.68
4	A	0.1304	-0.67	11	A	0.0470	-0.79
	B	.1033	-.59		B	.1236	-.59
	C	.1597	-.68		C	.0232	-1.14
5	A	0.1648	-0.83	12	A	0.0809	-0.77
	B	.4296	-.47		B	.1459	-.61
	C	------	-----		C	.059	-1.03
6	A	0.2367	-1.02	13	A	0.1036	-0.74
	B	.3424	-.65		B	.2159	-.56
	C	.3626	-.47		C	------	-----
7	A	0.2628	-0.85				
	B	.3673	-.58				
	C	.3076	-.49				

[a]The location numbers are not related to any specific locations on the vane surfaces. The specific location of each thermocouple on each vane can be determined from fig. 4 together with fig. 10, 11, or 12.

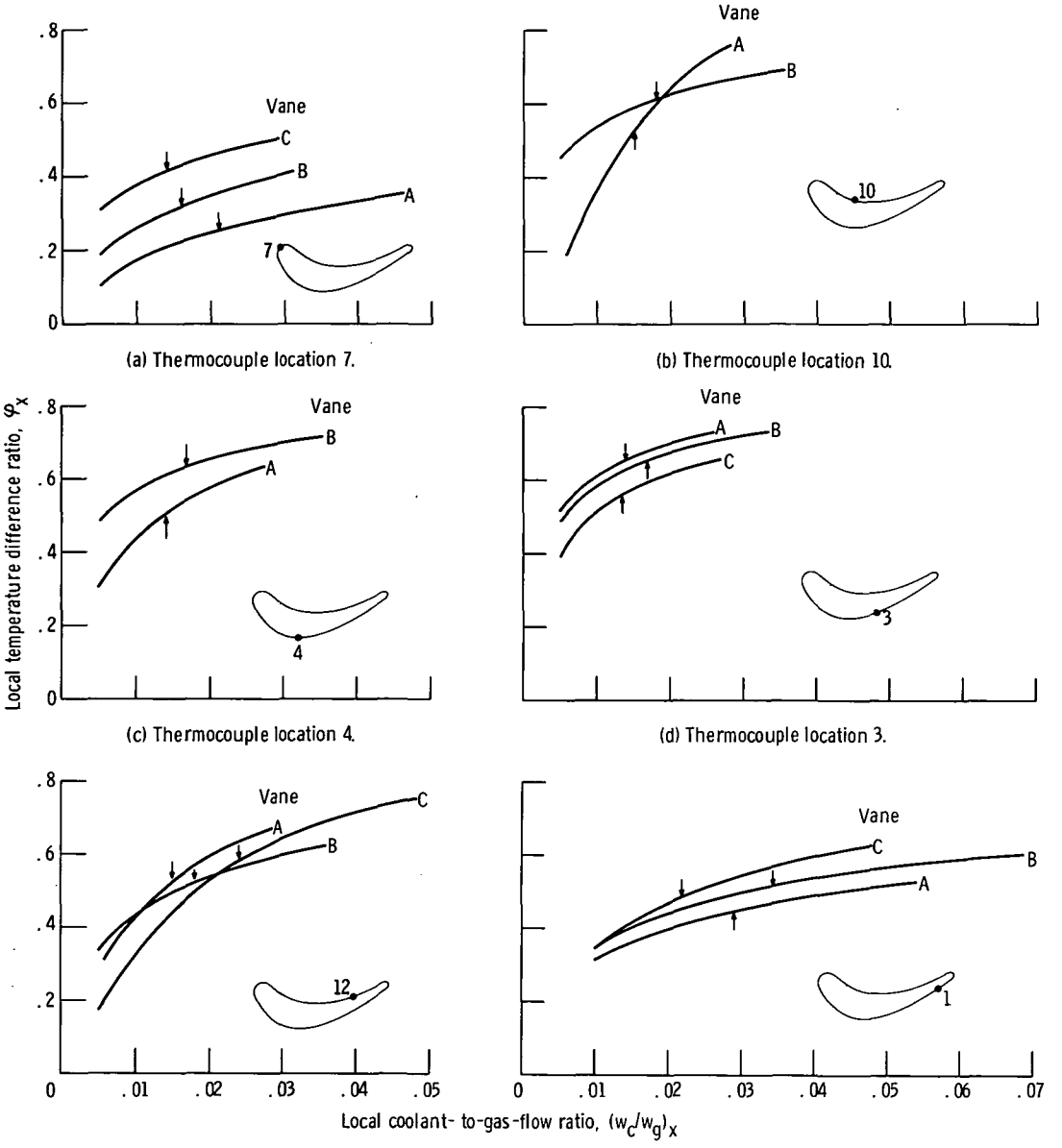

(a) Thermocouple location 7.

(b) Thermocouple location 10.

(c) Thermocouple location 4.

(d) Thermocouple location 3.

(e) Thermocouple location 12.

(f) Thermocouple location 1.

Figure 8. - Comparison of local temperature difference ratio φ_x against local coolant flow ratio $(w_c/w_g)_x$. Arrow represents 5 percent total coolant flow at $T_{ci} = 920$ K (1200° F).

Midchord region φ values. - Representative local φ values for the midchord region are shown in figures 8(b) to (d). The local coolant flow ratio for both vanes A and B is 48 percent of the trailing edge flow ratio for the suction surface chordwise passages, and 52 percent for the pressure surface chordwise passages. Vane C has a comparable thermocouple at location 3 only. The local coolant flow ratio for vane C at this point is 57 percent of the coolant flow to the midchord region.

Figure 8(b) shows the local φ values on the pressure surface for vanes A and B for thermocouple location 10. On vane A, the thermocouple is located downstream of the film cooling holes, but before the start of the chordwise passages. On vane B, this corresponding thermocouple location is 11 equivalent passage diameters from the start of the chordwise passages. The curves in this figure intersect at a local coolant flow ratio of about 0.018. The local φ values of vane A are higher than those of vane B above the intersection, and lower than those of vane B below the intersection. This particular region in vane A utilizes film cooling on the external surface but has relatively ineffective convection cooling on the internal surface. Figure 8(b) indicates that at low coolant flow ratios, the cooling configuration of vane B is more effective than that of vane A. At high coolant flow ratios, film cooling is more effective.

Figure 5 illustrates the reason for the apparent ineffectiveness of film cooling at low coolant flow ratios. As shown in the figure, the coolant flow through the film cooling holes in the pressure surface approaches zero as the ratio of coolant inlet pressure to turbine inlet pressure approaches 0.88. For thermocouple location 10, this pressure ratio corresponds to a local coolant flow ratio of 0.008 at a coolant inlet temperature of 922 K (1200° F). Obviously, for the case of zero film cooling flow, vane B with chordwise passages should be more effective than vane A without chordwise passages.

As the ratio of coolant inlet pressure to turbine inlet pressure increases above 0.88, the proportion of local coolant flow to the total coolant flow through the pressure surface film cooling holes increases rapidly. Eventually, the cooling effectiveness due to film cooling on vane A, even with poor internal convective cooling, was greater than the cooling effectiveness of vane B, which had good internal convection cooling, but no film cooling.

Figure 8(c) shows a similar comparison of the cooling effectiveness of vane A and vane B on the suction surface, for thermocouple location A. In this figure, the effectiveness of the nonfinned cooling configuration of vane A is shown to be less than that of the finned cooling configuration of vane B throughout the range of local coolant flow ratios. The reason for the relative ineffectiveness of vane A is attributed to its poor internal cooling as compared to that of vane B, which has a fin effectiveness factor of 3. Calculations show that if the fin effectiveness factor of vane B were to be eliminated, the cooling effectiveness of vane A would be higher than that of vane B throughout the range of coolant flow ratios shown.

Figure 8(d) compares the cooling effectiveness of vanes A, B, and C on the suction surface, for thermocouple location 3. The higher cooling effectiveness of vane A is attributed to the entrance effect on the coolant side heat transfer coefficient, as the coolant enters the chordwise passages. Calculations show that if this entrance effect were eliminated, the cooling effectiveness of vane A would be about the same as that of vane B in spite of the fact that vane A has film cooling.

The cooling effectiveness of vane B is greater than that of vane C throughout the range of coolant flow ratios at this location. From the comparison given in figure 8(d), impingement cooling is less effective than the chordwise passages, at least for this particular location and for the geometries represented by vanes B and C. The effectiveness of the impingement cooling on vane C at this point may have been substantially lowered by the presence of cross flow.

Trailing edge φ values. - The local φ curve for thermocouple location 12 is shown in figure 8(e), plotted against the local flow ratios. Thermocouple location 12 is at a point just before the end of the chordwise passages on vanes A and B on the pressure surface. On vane C, the thermocouple is actually located about 0.56 centimeter (0.22 in.) closer to the leading edge, but nevertheless is included in the comparison. The thermocouple on vane C is located downstream of the film cooling slots (fig. 5). The split trailing edge of vane C also contains 5 rows of pin fins. For vanes A and B, the local flow is the portion of the total flow which travels through the pressure surface chordwise passages (52 percent of the trailing edge flow). For vane C, the local flow is the flow through the split trailing edge.

The higher cooling effectiveness of vane A as compared with that of vane B is again attributed to the film cooling, still effective at this point on the pressure surface. The φ values for vane C reflect the combined effects of film cooling and pin fins in the trailing edge. In figure 8(e), the φ values for vanes A and C generally increase more rapidly at lower coolant to gas flow ratios, and surpass the local φ values of vane B at higher flow ratios. This is consistent with the film cooling flow characteristics on the pressure surface, shown in figures 5 and 7.

Figure 8(f) shows the local φ values of vanes A, B, and C on the suction surface of the trailing edge for thermocouple location 1. The curve for vane B, without film cooling, is higher than the curve for vane A over the entire range of coolant flow ratios inspite of the fact that, for a given coolant flow ratio, vane A has a higher coolant side heat transfer coefficient. The higher coolant side heat transfer coefficient is due to the fact that the width of the split trailing edge of vane A is 0.051 centimeter (0.020 in.) as compared to 0.076 centimeter (0.030 in.) for vane B. Consequently, the flow per unit area of vane A is higher than that of vane B for the same coolant flow rate.

The lower cooling effectiveness of vane A compared to that of vane B might be due to a detrimental effect of film cooling air injection near the leading edge of the suction

surface of vane A. The cooling air injection to the gas stream near the leading edge on the suction surface might have the effect of increasing the heat flux to vane A at this particular location. It is speculated that the injection of film cooling air might have triggered a local separation of the boundary layer on the suction surface trailing edge, where an adverse pressure gradient exists (ref. 12).

Vane C displays in figure 8(f) a higher cooling effectiveness than does vane B. However, if the cooling effectiveness of vane C is reduced by taking into account the effect due to the presence of the pin fins in the trailing edge, the resulting cooling effectiveness of vane C with film cooling appears to be lower than that of vane B, which has no film cooling. The data from vane C, which has film cooling flow exiting from slots on the suction surface at a point downstream of the midchord region, indicate that film cooling may be ineffective, or even detrimental, near the suction surface trailing edge.

Comparison of Average Temperature Difference Ratio

While the local φ values are important in knowing the location of the hottest metal temperature and the chordwise temperature gradient in a vane, the average temperature of a vane is also of interest, because it affects the life of the hardware.

The average φ values for vanes A, B, and C, based on an integrated average metal temperature, are presented in figure 9.

On the basis of the integrated average metal temperature, the φ values for vane B are highest at low w_c/w_g ratios, followed by vane C and vane A. In this region, the chordwise passages of vane B are evidently more effective than vane C with impingement cooled midchord, film cooling and pin fins in the trailing edge, and vane A with chord-

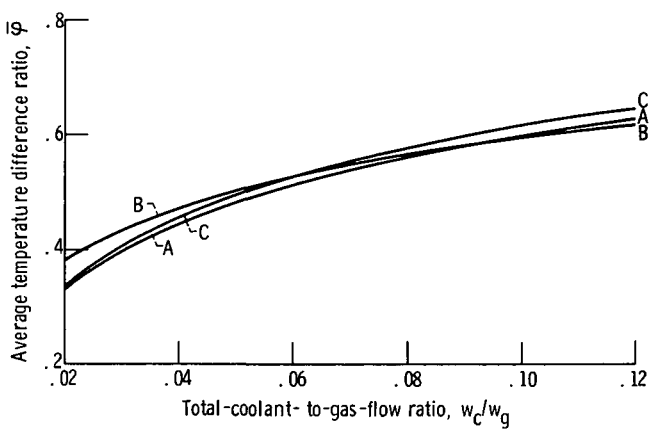

Figure 9. - Comparison of average temperature difference ratio for vanes A, B, and C.

wise passages and film cooling aft of the leading edge. At the higher w_c/w_g ratios, the φ values for vane C are the highest, followed by those for vane A and vane B.

It is noted that on the basis of the average metal temperatures, the φ values of the three vanes are relatively close to each other throughout the range of the w_c/w_g ratios, which indicates that the performance of the three vanes on an average basis was about the same.

Analytically Improved Cooling Performance

The original design for vane A shows that the midchord region is overcooled relative to the leading edge region. Consequently, the design can be improved by moving the row of impingement nozzles closer to the leading edge and by redistributing the flow similar to vane B. In addition, the chordwise fins of vane A were extended over the entire midchord region. Reference 3 presents more information concerning a possible revised design for vane A.

The chordwise temperature distributions for vane A and a modified vane A are compared in figure 10. The curves are based on a coolant flow ratio of 0.05, a coolant inlet temperature of 922 K (1200° F), and a turbine inlet temperature of 1515 K (2268° F). For the design conditions stated, the leading edge hotspot temperature is reduced by 144 K (261° F) to 1278 K (1840° F), and the average temperature is reduced by 6 K (11° F) to 1231 K (1756° F). The maximum to minimum temperature difference is 292 K (525° F) for the original design compared to 110 K (198° F) for the revised design. The required ratio of coolant inlet pressure to turbine inlet pressure, which is necessary for

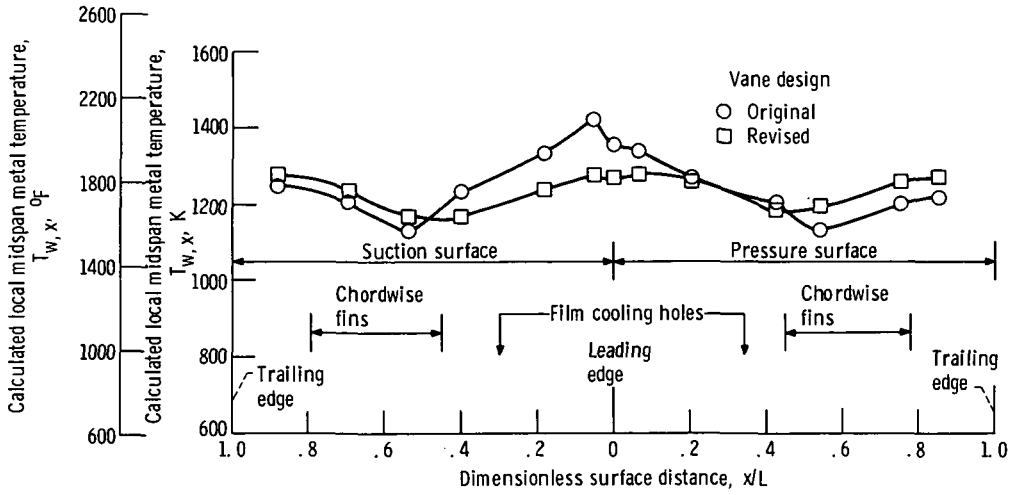

Figure 10. - Comparison of calculated chordwise temperature distributions for vane A and modified vane A based on turbine inlet temperature of 1515 K (2268° F), coolant inlet temperature of 922 K (1200° F), and coolant- to-gas-flow ratio of 0.05.

the vane to pass a 0.05 coolant- to-gas-flow ratio at 922 K (1200° F), is reduced from 1.11 to 1.00. The flow distribution changes to 36.6 percent to the suction surface film cooling holes, 26.4 percent to the pressure surface film cooling holes, and 37 percent to the afterbody region compared with the original distribution of 18, 24.4, and 57.6 percent, respectively.

Vane B was designed to operate at a maximum wall temperature of 1278 K (1840° F), a coolant inlet temperature of 922 K (1200° F), and a coolant- to-gas-flow ratio of 0.05, which are the same as those used to design vane A. Experimental flow data, extrapolated to this design point, have shown that a coolant- to-gas-flow ratio of 0.05 will split 31.5 percent to the leading edge region and 68.5 percent to the afterbody region. This flow distribution would have resulted in leading edge wall temperatures in excess of 1278 K (1840° F) had the vane actually been tested at any temperatures above 1426 K (2107° F).

The midspan temperature distribution for vane B (fig. 11) shows that the chordwise finned region is overcooled relative to the leading edge. This vane design could again be improved by changing certain critical dimensions so that a greater proportion of the coolant would be distributed to the hotter leading edge area. The critical dimensions which would change are the trailing edge slot width and the impingement nozzle diameter.

Figure 6 shows the internal cooling air distribution for vane B, derived entirely from cold flow data. This figure alone is adequate for determining the flow distribution for an actual engine heat transfer test point, since the coolant inlet pressure and the turbine inlet pressure are measured. However, this figure is not sufficient for determining the flow distribution for a revised cooling configuration, where the pressure ratio is unknown. In order to obtain the flow distribution for the revised design, figure 6 was

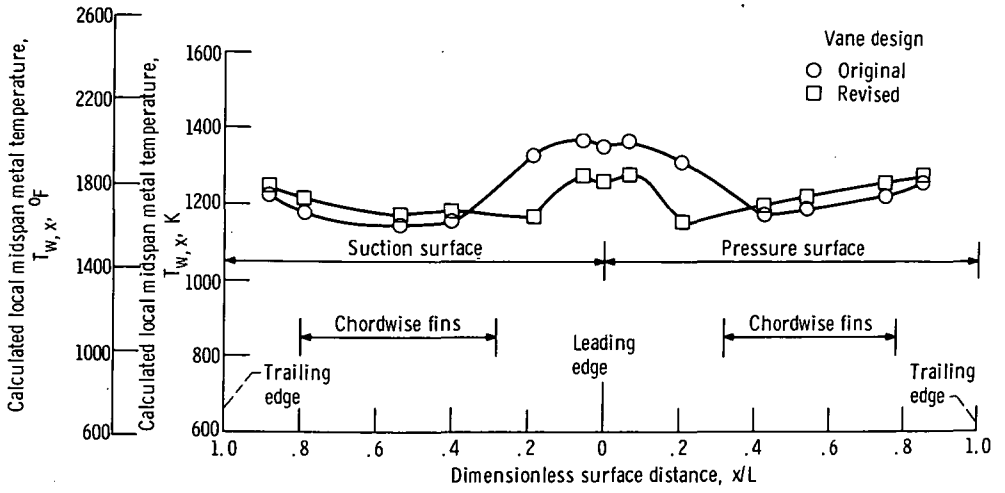

Figure 11. - Comparison of calculated chordwise temperature distributions for vane B and modified vane B based on turbine inlet temperature of 1552 K (2334° F), coolant inlet temperature of 922 K (1200° F), and coolant- to-gas-flow ratio of 0.05.

used in conjunction with engine data relating the coolant inlet temperature and coolant-to-gas-flow ratio with the ratio of coolant inlet pressure to turbine inlet pressure.

The vane can be further improved by changes in design other than just redistribution of flow. One example of such a change, used in the revised design, was to optimize the leading edge impingement geometry. Reference 5 states that maximum heat transfer occurs when the spacing between the semicylinder and a linear array of circular jets is approximately two equivalent slot widths if the center to center spacing of the jets is 1.66 nozzle diameters. The original vane has a spacing of 8.2 equivalent slot widths, with a center-to-center jet spacing of 1.6 nozzle diameters.

Calculated temperature distributions for both the original and revised vanes are presented in figure 11. These temperature distributions are obtained by evaluating the local temperature difference ratios found in table I, which are based on the local coolant-to-gas-flow ratio.

For a turbine inlet total gas temperature of 1552 K (2334^{o} F), a coolant temperature of 922 K (1200^{o} F), and a coolant- to-gas-flow ratio of 0.05, the calculated maximum temperature of the revised vane is 1278 K (1840^{o} F). These calculations show that the leading-edge temperature is reduced by 91 K (165^{o} F) and the average temperature is reduced by 20 K (36^{o} F) relative to the original design. The maximum to minimum temperature difference is 225 K (404^{o} F) for the original design compared to 70 K (114^{o} F) for the revised design. The required ratio of coolant inlet pressure to turbine inlet pressure, which is necessary for the vane to pass a 0.05 coolant-to-gas flow ratio at 922 K (1200^{o} F), will be reduced from 1.26 to 1.0. The flow distribution will change to 52.3 percent to the leading edge region and 47.7 percent to the afterbody region compared with the original distribution of 31.5 and 68.5 percent, respectively.

The chordwise temperature distribution for vane C is shown in figure 12 for the same coolant conditions and a gas temperature of 1519 K (2275^{o} F). Since this vane was

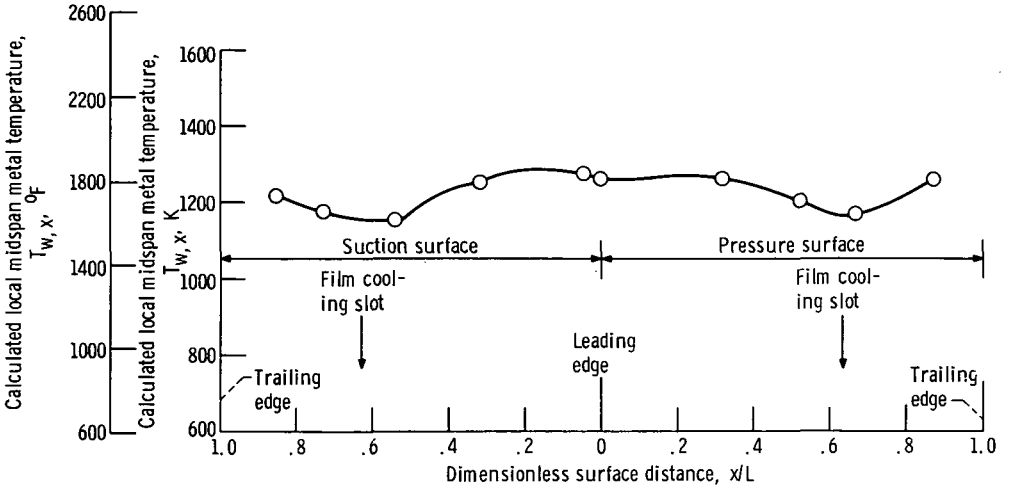

Figure 12. - Calculated chordwise temperature distribution for vane C based on turbine inlet temperature of 1543 K (2317^{o} F), coolant inlet temperature of 922 K (1200^{o} F), and coolant- to-gas-flow ratio of 0.05.

not designed and fabricated by NASA, whereas the two other vanes were, no attempt has been made to improve the design. The resulting maximum wall temperature is 1278 K (1840° F), and the corresponding maximum temperature difference is 126 K (226° F), while the average temperature is 1225 K (1743° F).

Vane Temperature Potential

The maximum allowable turbine inlet gas temperature for a given coolant flow ratio and a given coolant temperature is limited by the maximum allowable metal temperature of the vane, if the temperature gradient in the vane is acceptable. A comparison of the maximum allowable turbine inlet temperatures for vanes A, B, and C, as well as for the redesigned versions of vanes A and B, at a coolant- to-gas-flow ratio of 0.05 is presented in figure 13. The turbine inlet temperature, shown as a function of the total coolant- to-gas-flow ratio, is calculated by using a maximum metal temperature of 1278 K (1840° F). Figure 13 shows that the maximum allowable turbine inlet temperature for vane C is higher than for either vane B or vane A. In the modified designs for a coolant flow ratio of 0.05, the maximum allowable turbine inlet temperature for vane B is 33 K (59° F) higher than for vane C, which in turn is 4 K (7° F) higher than for the modified design of vane A. Further design improvements such as addition of plate fins in the leading edge and pin fins in the trailing edge are possible for the modified versions of vanes A and B, and the corresponding maximum allowable turbine inlet temperatures would be higher.

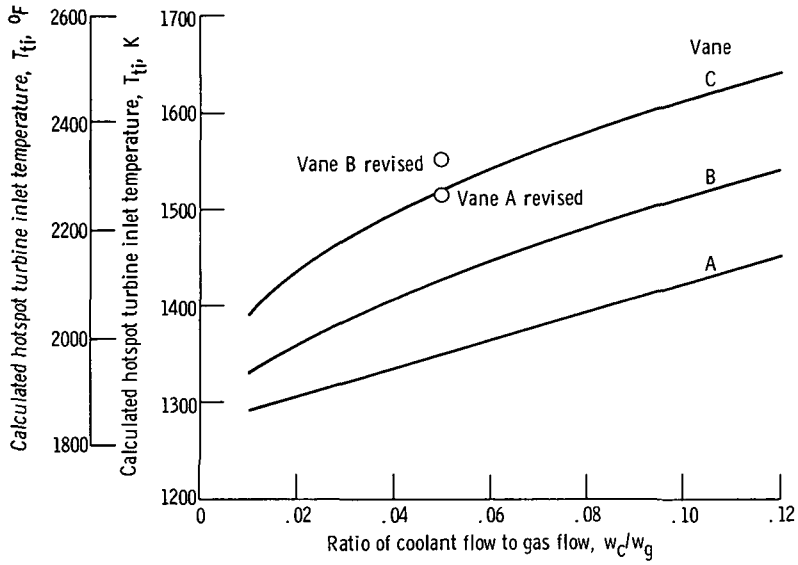

Figure 13. - Calculated hotspot turbine inlet temperature as function of coolant flow ratio for hotspot vane temperature of 1278 K (1840° F) and coolant inlet temperature of 922 K (1200° F).

TABLE III. - VANE PERFORMANCE COMPARISON BETWEEN ORIGINAL AND REVISED DESIGNS

	Vane configuration				
	A		B		C
	Original	Revised	Original	Revised	
Coolant- to-gas-flow ratio	0.05	0.05	0.05	0.05	0.05
Coolant inlet temperature, K (^{o}F)	922 (1200)	922 (1200)	922 (1200)	922 (1200)	922 (1200)
Maximum vane temperature, K (^{o}F)	1422 (2101)	1278 (1840)	1369 (2005)	1278 (1840)	1278 (1840)
Average vane temperature, K (^{o}F)	1237 (1767)	1231 (1756)	1237 (1766)	1217 (1730)	1224 (1743)
Maximum vane temperature difference, K (^{o}F)	292 (525)	110 (198)	225 (404)	70 (114)	126 (226)
Hotspot gas temperature, K (^{o}F)	1515 (2268)	1515 (2268)	1552 (2334)	1552 (2334)	1519 (2275)
Coolant flow to leading edge, percent	42.4	63	31.5	52.3	28.2
Coolant flow through suction surface slot, percent	18.0	36.6	----------	----------	11.2
Coolant flow through pressure surface slot, percent	24.4	26.4	----------	----------	13.6
Coolant flow through split trailing edge, percent	57.6	37	68.5	47.7	47
Ratio of coolant-inlet- to turbine-inlet pressure	1.11	1	1.26	1	1.25

Table III presents a comparison of temperatures, flowrates, and pressure ratios for the three original and the two revised vane configurations. The temperatures listed in this table demonstrate that the two revised vane designs are substantially improved over the respective original designs. Also demonstrated in the table is the fact that the revised vane B design is a better design than either the revised vane A configuration or the vane C configuration.

Comparison of Impingement Correlations and Experimental Data

Average leading edge coolant Nusselt numbers were determined for the three vanes reported by use of measured temperatures and equations (9) to (13). The coolant properties used in these calculations were evaluated at the coolant inlet temperature, as was generally done in impingement correlations reported in literature. These data are presented in figure 14 as a function of Reynolds number based on twice the equivalent slot width. Also shown in the figures are the modified empirical correlations of equations (2) to (5).

The data from vane A for a row of holes with a z_n/b_{es} of 10.6 are shown in figure 14(a). The results of this comparison suggest that at large z_n/b_{es} ratios, a row of holes may perform more like a slot, since these data are correlated by a slot correlation of reference 6, modified for a nonoptimum z_n/b_{es}. The experimental data are within ±10 percent of this correlation. The data are also correlated within ±10 percent by the equation of reference 4.

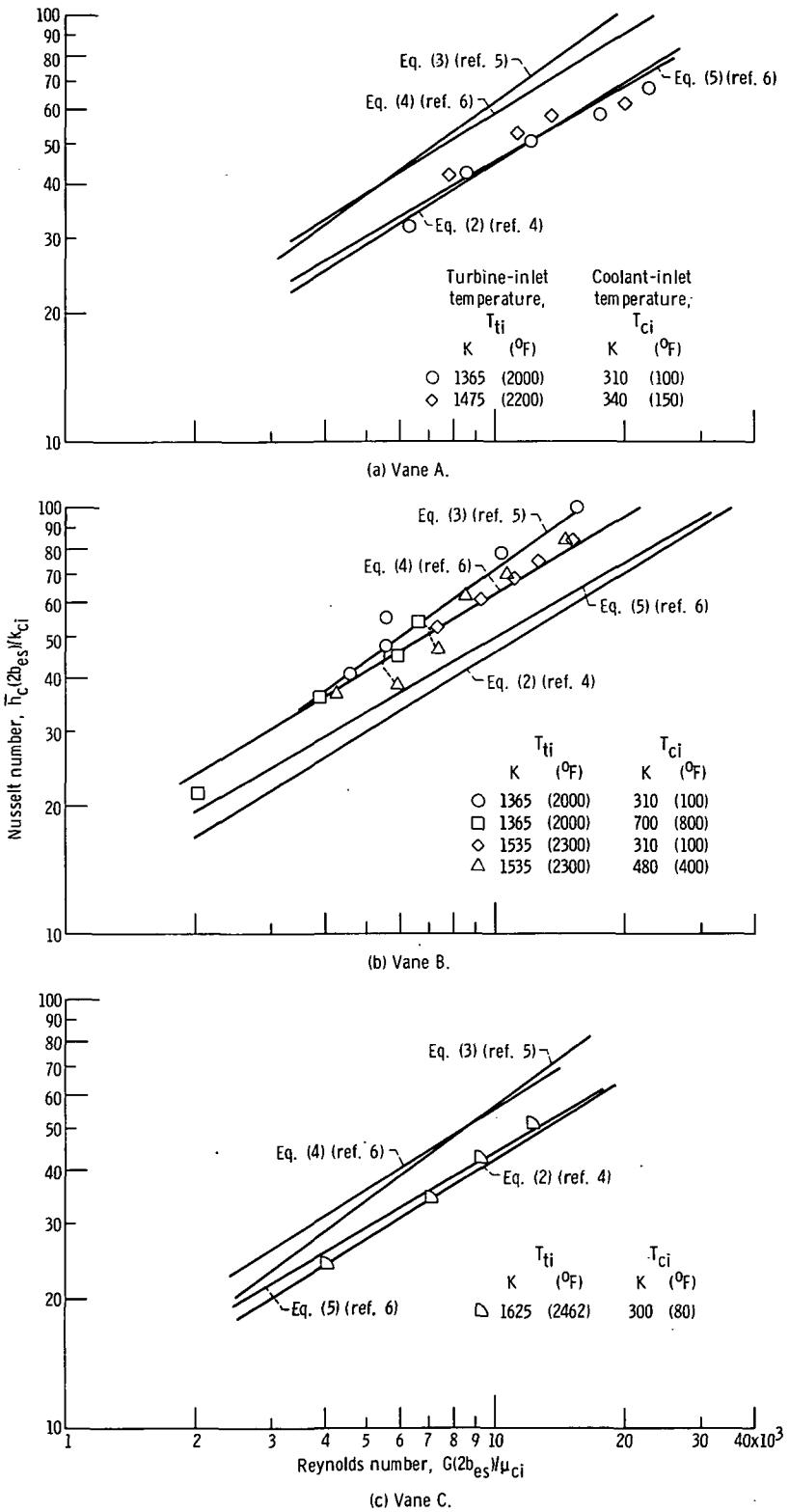

Figure 14. - Comparison of Nusselt number as a function of Reynolds number for an impingement cooled leading edge based on experimental data and some available correlations, modified for the geometries being considered.

Vane B had a similar row of holes at the leading edge as vane A except that the z_n/b_{es} ratio was 8.2. The data for vane B are shown in figure 14(b). These data are correlated within ±10 percent by a modified correlation, for impingement flow through holes, from reference 6, and within ±14 percent by the correlation of reference 5, with the exception of three ambient temperature coolant data points which were considerably higher than the other data. The correlations are evaluated by using the geometries of vane B.

The leading edge of vane C is also impingement cooled, but by a row of slots instead of holes as in vanes A and B. The data shown in figure 14(c) are limited to the ambient coolant temperature. These data compare favorably with the modified slot correlation of reference 6, and are within ±10 percent of this correlation. The data are also within 10 percent of the correlation of reference 4.

The evaluation of impingement heat transfer coefficients for vane C does not take into account the fin effectiveness. Such a correction applied to the experimental data could cause the data to fall below the correlation lines in figure 14(c).

SUMMARY OF RESULTS

The following summarizes the results obtained from the comparison of three vanes tested at the Lewis Research Center.

1. The film cooled vane having two rows of holes just aft of the leading edge on the pressure surface was more effective in the midchord region, even with ineffective convection cooling, than the convection cooled vane having a fin effectiveness factor of 3; and it was partially effective far downstream, near the trailing edge.

2. The film cooled vane having one row of holes just aft of the leading edge on the suction surface was less effective in the midchord region, with ineffective internal convection cooling, than the convection cooled vane having a fin effectiveness factor of 3; and it was ineffective, and perhaps even detrimental, far downstream, near the trailing edge.

3. At low coolant- to-gas-flow ratios, the vane with the chordwise passages and no film cooling has the highest average cooling effectiveness. At high coolant- to-gas-flow ratios, the vane with impingement cooled midchord and pin fins in the trailing edge has the highest average cooling effectiveness. The three vanes compared were nearly equal in cooling effectiveness throughout the range of coolant- to-gas-flow ratios, based on the average metal temperature; this indicates that on an average basis the three vanes were similar in performance.

4. Two of the vanes compared in this report were redesigned. Based on calculations the redesigned version show a much improved chordwise temperature distribution. The following table compares the more important parameters resulting from the design study:

	Vane A				Vane B			
	Original		Revised		Original		Revised	
Coolant- to-gas-flow ratio	0.05		0.05		0.05		0.05	
Turbine inlet temperature, K (^{o}F)	1515	(2268)	1515	(2268)	1552	(2334)	1552	(2334)
Coolant inlet temperature, K (^{o}F)	922	(1200)	922	(1200)	922	(1200)	922	(1200)
Maximum vane temperature, K (^{o}F)	1422	(2101)	1278	(1840)	1369	(2005)	1278	(1840)
Maximum temperature difference, K (^{o}F)	292	(525)	110	(198)	225	(404)	70	(114)

5. At the leading edge, impingement cooling, combined with plate fins, was more effective in reducing metal temperatures than were two other configurations without plate fins.

6. Average impingement heat transfer coefficients around the leading edge, calculated by using experimental temperatures, were compared with some existing impingement heat transfer correlations. These calculated values agreed within ±10 percent with the closest impingement heat transfer correlation.

Lewis Research Center,
National Aeronautics and Space Administration,
Cleveland, Ohio, June 19, 1972,
501-24.

APPENDIX - SYMBOLS

A	constant obtained from experimental data
B	constant obtained from experimental data
b_{es}	equivalent slot width, $n\pi d_n^2/4L_v$
c_n	center-to-center distance between nozzles
D	diameter
D_h	hydraulic diameter
d_n	diameter of nozzle
G	mass velocity, ρV
h	heat transfer coefficient
k	thermal conductivity
L	surface length between leading edge and trailing edge for either the pressure or the suction surface
L_{fin}	effective height of chordwise passages
L_v	span length of vane
ℓ	surface length from stagnation point
m	surface-to-surface distance between adjacent fins
Nu	Nusselt number
n	number of impingement nozzles
P	pressure
Pr	Prandtl number
Re	Reynolds number
r	radius
S	surface area
T	temperature
V	velocity
w	weight flow
x	distance from leading edge to point on vane surface
z_n	distance from nozzle to leading edge surface
θ	angular distance in degrees from stagnation point

μ dynamic viscosity

ρ density

τ metal thickness of chordwise passages

φ temperature difference ratio, $(T_{ti} - T_w)/(T_{ti} - T_{ci})$

Subscripts:

a arrival

av average

c coolant

cas cascade

ci coolant inlet

eng engine

f film

fin fin

g gas

i inside

le leading edge

max maximum

n nozzle

o outside

ti turbine inlet

w wall

x thermocouple location number

1 original design

2 modified design

REFERENCES

1. Gladden, Herbert J.; Gauntner, Daniel J.; and Livingood, John N. B.: Analysis of Heat-Transfer Tests of an Impingement-Convection- and Film-Cooled Vane in a Cascade. NASA TM X-2376, 1971.

2. Dengler, Robert P.; Yeh, Frederick C.; Gauntner, James W.; and Fallon, Gerald E.: Engine Investigation of Air-Cooled Turbine Rotor Blade Incorporating Impingement-Cooled Leading Edge, Chordwise Passages, and a Slotted Trailing Edge. NASA TM X-2526, 1972.

3. Gauntner, James W.; Lane, Jan M.; Dengler, Robert P.; and Hickel, Robert O.: Experimental Heat Transfer and Flow Results of a Chordwise-Finned Turbine Vane with Impingement, Film, and Convection Cooling. NASA TM X-2472, 1972.

4. Burggraf, F.: Average Heat Transfer Coefficients with a Row of Air Jets Discharging into a Half Cylinder. M.S. Thesis, Univ. of Cincinnati, 1967.

5. Metzger, D. E.; Yamashita, T.; and Jenkins, C. W.: Impingement Cooling of Concave Surfaces with Lines of Circular Air Jets. Paper 68-WA/GT-1, ASME, Dec. 1968.

6. Jenkins, C. W.; and Metzger, D. E.: Local Heat Transfer Characteristics of Concave Cylindrical Surfaces Cooled by Impinging Slot Jets and Lines of Circular Jets with Spacing Ratios 1.25 to 6.67. Rep. ME-694, Arizona State Univ., May 1969.

7. Gladden, Herbert J.; and Yeh, Frederick C.: Comparison of Heat-Transfer Test Data for a Chordwise-Finned Impingement-Cooled Turbine Vane Tested in a Four-Vane Cascade and Research Engine. NASA TM X-2595, 1972.

8. Calvert, Howard F.; Cochran, Reeves P.; Dengler, Robert P.; Hickel, Robert O.; and Norris, James W.: Turbine Cooling Research Facility. NASA TM X-1927, 1970.

9. Livingood, John N. B.; Ellerbrock, Herman H.; and Kaufman, Albert: NASA Turbine Cooling Research Status Report, 1971. NASA TM X-2384, 1971.

10. Livingood, John N. B.; and Brown, W. Byron: Analysis of Spanwise Temperature Distribution in Three Types of Air-Cooled Turbine Blade. NACA TR 994, 1950.

11. Clark, John S.; Richards, Hadley T.; Poferl, David J.; and Livingood, John N. B.: Coolant Pressure and Flow Distribution Through an Air-Cooled Vane for a High-Temperature Gas Turbine. NASA TM X-2028, 1970.

12. Gladden, Herbert J.; Dengler, Robert P.; Evans, David G.; and Hippensteel, Steven A.: Aerodynamic Investigation of Four-Vane Cascade Designed for Turbine Cooling Studies. NASA TM X-1954, 1970.

NASA-Langley, 1972 —— 33 E-6948

"The aeronautical and space activities of the United States shall be conducted so as to contribute . . . to the expansion of human knowledge of phenomena in the atmosphere and space. The Administration shall provide for the widest practicable and appropriate dissemination of information concerning its activities and the results thereof."

—NATIONAL AERONAUTICS AND SPACE ACT OF 1958

NASA SCIENTIFIC AND TECHNICAL PUBLICATIONS

TECHNICAL REPORTS: Scientific and technical information considered important, complete, and a lasting contribution to existing knowledge.

TECHNICAL NOTES: Information less broad in scope but nevertheless of importance as a contribution to existing knowledge.

TECHNICAL MEMORANDUMS: Information receiving limited distribution because of preliminary data, security classification, or other reasons. Also includes conference proceedings with either limited or unlimited distribution.

CONTRACTOR REPORTS: Scientific and technical information generated under a NASA contract or grant and considered an important contribution to existing knowledge.

TECHNICAL TRANSLATIONS: Information published in a foreign language considered to merit NASA distribution in English.

SPECIAL PUBLICATIONS: Information derived from or of value to NASA activities. Publications include final reports of major projects, monographs, data compilations, handbooks, sourcebooks, and special bibliographies.

TECHNOLOGY UTILIZATION PUBLICATIONS: Information on technology used by NASA that may be of particular interest in commercial and other non-aerospace applications. Publications include Tech Briefs, Technology Utilization Reports and Technology Surveys.

Details on the availability of these publications may be obtained from:

SCIENTIFIC AND TECHNICAL INFORMATION OFFICE

NATIONAL AERONAUTICS AND SPACE ADMINISTRATION

Washington, D.C. 20546